Cotton Dust Particle Size Distribution in Oil Mills

D.P. THIBODEAUX, Southern Regional Research Center[1], PO Box 19687, New Orleans, LA 70179

ABSTRACT

Analytical procedures have been developed for characterizing the size and shape of cotton dust particulates collected by the vertical elutriator (VE) sampler. Data are reported for dust distributions on VE filters collected from different processing areas (cleaning, delintering, hulling, and baling) in cottonseed oil mills. Results of particle volume distributions obtained with a Coulter counter are compared with data obtained from an image-analysis system designed to classify cotton dust into fibrous and nonfibrous (particulate) components. The image-analysis data include distributions of the lengths and widths of fibers and the areas and diameters of particles present on the VE filters. In many of the locations studied, a considerable amount of the total dust sampled can be attributed to lint, lint fragments, and also to particles significantly larger than 15 μm diameter.

INTRODUCTION

This work is part of a cooperative study between USDA-SEA-AR and Texas Tech University aimed at characterizing occupational dust control equipment used in cottonseed oil mills and providing engineering specifications on such equipment. The vertical elutriator (VE) air sampler (1) was used in this study to measure the concentrations of respirable cotton dust in the air at major processing locations in selected cottonseed oil mills.

The major objective of the research reported herein has been to characterize the size and nature of the particulates collected on filters from VE operated especially for this purpose. This type of information is essential to the development of engineering specifications for improved control of fugitive cotton dusts associated with cottonseed oil mill processing.

Scope

This research has included (a) development of a method to distinguish microscopically between lint-like fibers or fiber fragments and nonlint (more circular) particles deposited on VE filters; (b) comparison of particle size distributions obtained from Coulter counter analysis with those obtained from microscopic image analysis of replicate VE filter samples; and (c) evaluation of the performance of the VE sampler in a cottonseed oil mill relative to the criteria of sampling respirable nonlint dusts less than 15 μm in diameter (2).

Background

Matlock et al. (3) reported results of measurement of VE dust levels in 5 Texas cottonseed oil mills processing stripper-harvested cotton. Dust levels measured in the 4 major processing areas (cleaning, delintering, hulling and baling) averaged 6, 3.2, 4.3 and 1.7 mg/m^3, respectively. A Coulter counter was used to measure particle size distribution parameters of dust removed from the VE filters by ultrasonic washing in an electrolyte solution (4). The mass median diameter (MMD) and geometric standard deviation (GSD) of these dusts at the various areas were 9.42 ± 1.85 μm for cleaning, 8.66 ± 1.7 μm for delintering, 11.45 ± 1.74 μm for hulling, and 11.17 ± 1.7 μm for baling. These results were extended by Parnell and Matlock (5) who measured dust levels in seed and concluded that they greatly affect dust levels in the various work areas of cottonseed oil mills. These results were expanded on in a cooperative study between USDA-SEA-AR and Texas A&M University (6) in which 10 cottonseed oil mills that processed both picker- and stripper-harvested cotton were sampled (this study led to the SEA-Texas Tech program).

Although data on the nature of VE dust sampled in oil mills are apparently limited to the references cited, there are many references on performance of the VE in cotton textile mills. Bethea and Morey (7) reported that the VE collected a portion of lint when it operates at its specified flow rate of 7.4 L/min. They suggested that, to negate the possibility of lint collection, it would have to operate at ca. 4 L/min. Several other researchers (4,8,9) have also reported collection of lint and other particulates greater than 15 μm. Robert (10) has developed a semiempirical math model of the VE based on the assumption of turbulent separated flow which predicts sampling of particles much larger than 15 μm aerodynamic diameter. For these reasons, special attention was given to the fraction of lint present on the VE filters and also to what degree particulates greater than 15 μm were observed.

EXPERIMENTAL

Materials

Dust was collected on 3 different types of membrane filters. For the Coulter counter studies, the filter was a 37-mm diameter Nuclepore polycarbonate membrane with a 1.0-μm pore size. Filter media used for image analysis were either of the Millipore HP cellulosic membrane type, with a diameter of 37 mm and a pore size of 0.45 μm, or of the Nuclepore nitrocellulose membrane type, with a diameter of 37 mm and a pore size of 1.0 μm.

Equipment

All dust samples were obtained with either the General Metal Works or the Sierra Instruments Model 132 Cotton Dust Sampler (VE). A Model TA$_{II}$ Industrial Coulter counter was used, equipped with a measuring cell for which the aperture was 50 μm in diameter; this gives a population count of particles in a 0.5-mL sample in 15 channels, logarithmically distributed between 0.794 and 25.4 μm.

The image analyzer used was a Cambridge Instruments Quantimet System *23* interfaced to a *DEC PDP/1103* minicomputer and controlled via an interactive keyboard (11). The system used a Vidicon video scanner optically interfaced to an Olympus BH microscope and used a 720-line noninterlaced scan format digitized in such a way that the specimen comprised over 600,000 picture points (pixels). This electronic image was subjected to a detection process whereby features of interest were separated from the background on the basis of their gray level.

Approach

Two alternate techniques were applied to the dust size

[1]Southern Region, SEA, USDA.

distribution characterization. Samples were obtained at different locations using both carbonate and cellulosic membrane filter substrates. Dust collected on carbonate membranes could be ultrasonically removed in a methanol electrolyte solution and analyzed by the Coulter counter. This directly classifies the particles by volume and allows calculation of the mean and median particle diameters (assuming equivalent spherical particles) as well as the volume (mass) distributed as a function of particle diameter. The Coulter counter is calibrated with a suspension of 3.17 μm polystyrene spheres. This method is quite rapid and it measures the true particle volume, but it gives no indication of the actual shape or nature of the particle or whether the particles are subject to dissolving, swelling, or shattering in the liquid bath.

The cellulosic filters containing dust samples may be chemically clarified or dissolved and permanently mounted on slides for microscopic image analysis. In this process, the particles become electronically detected features that are counted, measured and classified according to one of the following geometrical criteria: area, perimeter, and length projected in an arbitrary direction. These parameters or mathematical functions of these parameters may be measured for each separate frame or field and retained in histogram form for all fields sampled. The same can be done with the cumulative sums of these feature parameters over the measurement fields.

A typical field of view of one of the microscopic dust samples displayed by the image analyzer scanner is shown in Figure 1. Obviously, both particles and fibers are included in the field. In order to discriminate between particles and fibers, 2 separate image analysis programs were developed to allow scanning for particles at high magnification (20× objective) and for fibers at low magnification (4× objective). When running the particle program, the operator uses an electronic light pen of the Quantimet's Editor module to reject fibrous features. This results in the selective electric detection of the particles which are shown in Figure 2 as being illuminated. The area of each particle detected is then measured in terms of the number of pixels it occupies and is automatically converted into μm^2 by calibration using a standard reticle. The major particle-size parameter determined by the program is the "effective circular diameter" (D_{ec}) which, as illustrated in Figure 3, is the diameter of a circle with the same area as the feature's measured area (A) defined as:

$$D_{ec} = 2 \cdot (A/\pi)^{0.5}. \quad [I]$$

The disadvantage of Equation I is that it is a 2-dimensional representation of a 3-dimensional particle. In order to compare more directly Coulter analysis results, it was necessary to make the rather bold assumption that the equivalent feature area circle may be rotated about a diameter to generate an equivalent spherical volume (V_{es}) given by $V_{es} = \pi (D_{ec})^3/6$. By substitution:

$$V_{es} = 4/(3(\pi)^{0.5}) \cdot (A)^{1.5}. \quad [II]$$

In the fiber program, the light pen is used to select fibrous features only, automatically rejecting particles. This is illustrated in Figure 4, which shows the selected fiber fragments illuminated and the rejected particles darkened. The ability of System 23 to measure automatically both the area and perimeter of each detected feature and calculate complex mathematical functions of both is used here to measure the effective length and width of each fiber. Using the logic of Robert (10), consider the serpentine object (fiber) shown in Figure 5, which has a total length L and an average width W. The fiber's area A = L × W and its perimeter is given by P = 2 (L + W). These equations

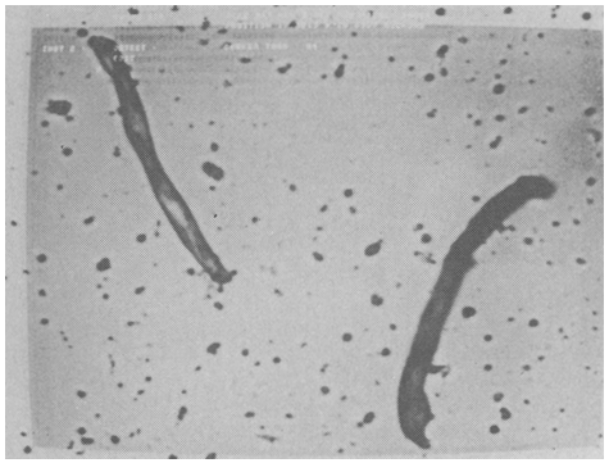

FIG. 1. Image analyzer display of VE cotton dust.

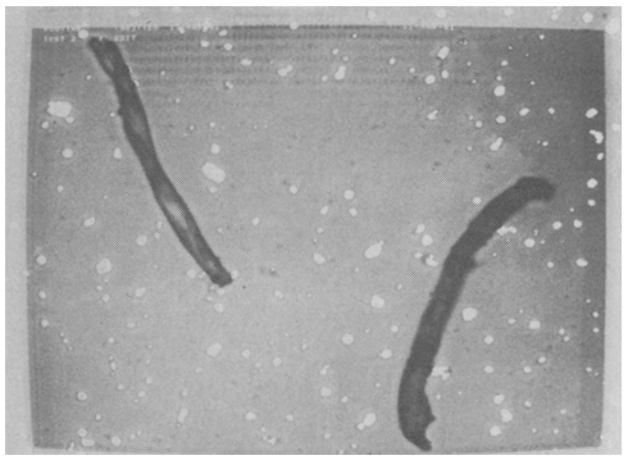

FIG. 2. Display of detected particles and rejected fibers.

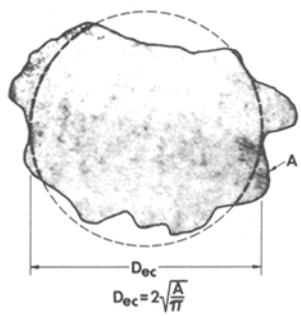

FIG. 3. The "Effective Circular Diameter" of a dust particle.

involve 2 measured parameters (A and P) and 2 unknown dimensions (L and W). Substituting for W in the second equation gives P = 2 (L + (A/L)) which will reduce to the quadratic form:

$$L^2 - PL/2 + A = 0. \quad [III]$$

The positive and negative roots of this equation are:

$$L = P/4 \pm (P^2 - 16\,A)^{0.5}/4. \quad [IV]$$

Simple physical considerations will lead to the conclusion that the positive root of Equation IV is the fiber length and

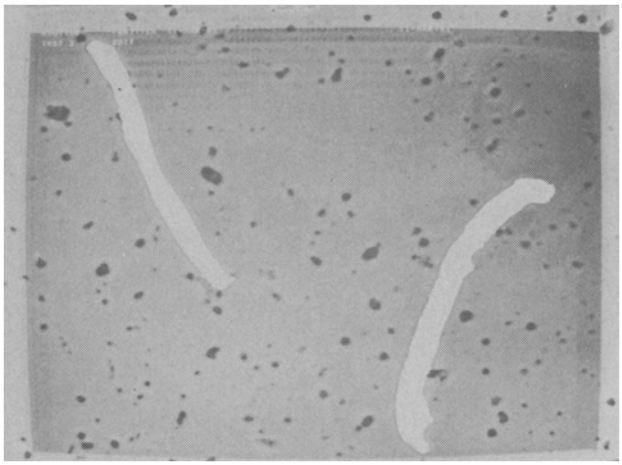

FIG. 4. Display of detected fibers and rejected particles.

the negative root is the fiber width. The fiber program is set up to solve for length and width, and to accumulate histogram information for all fibers measured. It also measures the sum of all fiber areas and volumes. The model used to calculate fiber volume assumes a fiber cross-section of width W and thickness (0.3·W) which results in the program calculating the fiber volume as:

$$V = 0.3 \cdot L \cdot W^2. \qquad [V]$$

Sample Preparations

The carbonate-membrane VE filters were placed in a clean beaker containing 200 mL of a solution of 5% lithium chloride in methanol, which was then immersed for 2 min in a 1-kW ultrasonic bath. The resulting suspension was filtered through a 400-mesh (37-μm) screen prior to being introduced into the 50-μm Coulter counting cell.

To clarify and mount the Millipore HP filters, (a) the filter was placed (particle side up) on a slide containing a solution of equal parts of hexane, 1,2-dichloroethane, and *p*-dioxane; (b) the filter was allowed to remain on the slide for 10 sec; (c) the filter was removed and placed (particle side up) on a second clean slide and allowed to dry for 1 min; (d) the slide and filter were inverted over a beaker filled to within 6 mm of its top with acetone; and (e) the slide was removed after 30 sec and allowed to stand at least 5 min before image analysis.

The best approach to preparing the Nuclepore nitrocellulose filter samples for image analysis is to dissolve one-fourth of the filter in ca. 0.7 mL of filtered and distilled amyl acetate. The resulting solution is evenly spread over the surface of a 75× 38 mm glass slide and allowed to dry for at least 1 hr.

RESULTS AND DISCUSSION

Data shown in Figure 6 represent a typical image-analysis histogram of numbers of particles in 20 logarithmically distributed intervals of D_{ec} as computed in Equation I. This curve has very much the bell-shaped characteristics of a normal probability distribution or, in this case, a log-normal distribution. Parameters of D_{ec} directly calculated from these data include mean particle diameter, $\bar{D}(P)$; the standard deviation about the mean, $\sigma(\bar{D})$; the number median diameter, $D_{½}(P)$; and the maximal measured particle diameter, $D_M(P)$. Values of the mass median particle diameter (MMD) and the geometric standard deviation (GSD) must be calculated by assuming a log-normal distribution and plotting the cumulative particle volume distribution on log

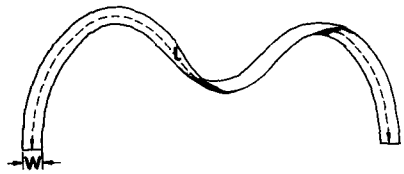

FIG. 5. Dimensional treatment of a typical lint fragment.

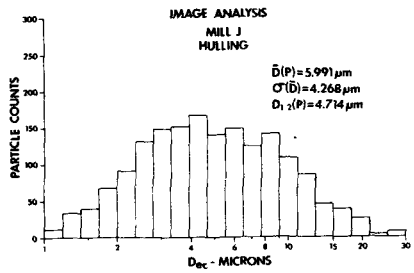

FIG. 6. Typical image analysis histogram of particle count distributed by log (D_{ec}).

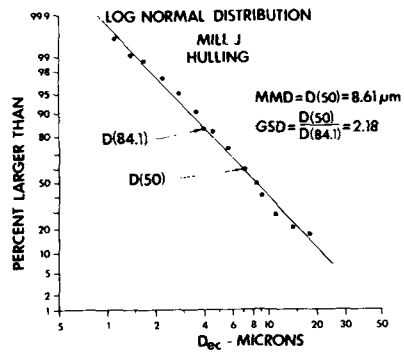

FIG. 7. Log probability distribution of cumulative particle volume vs log (D_{ec}).

probability paper as shown in Figure 7. A linear fit to these data is obtained and from it are determined the diameters at the 50% point D(50) and at the 84.1% point D(84.1). By definition, the MMD = D(50) and the GSD = D(50)/D(84.1). The degree of linearity indicates that these data are well approximated by a log-normal distribution.

The data from Figure 1 can be recalculated to give the differential percentage of total volume of each diameter interval as seen in Figure 8. This is accomplished by solving:

$$\Delta V(D) = (V_{es}(D)/\Sigma V_{es}(D)) \cdot 100, \qquad [VI]$$

where $\Sigma V_{es}(D)$ represents the total volume of all features in the specimen. Although the number distribution in Figure 6 was symmetric, the differential volume distribution is decidedly skewed toward the larger particle diameters. Thus, a few large particles will contribute greatly to the total volume (mass of the sample).

A replicate of the sample analyzed in Figures 1 and 4 obtained on a carbonate membrane filter and analyzed with the Coulter counter yielded the particle-count distribution shown in Figure 9. This population appears to be skewed toward the smaller particle sizes and to have a bimodal quality. This appearance is confirmed by the significantly lower distribution parameters than those shown in Figure 1. The differential volume distribution of these data is given

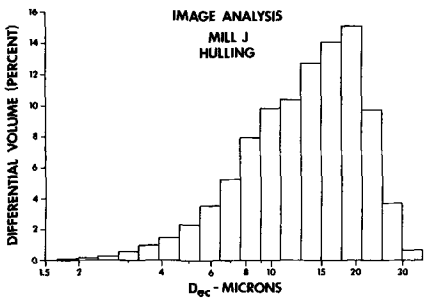

FIG. 8. Typical image analysis histogram of differential percentage total volume distributed by log (D_{ec}).

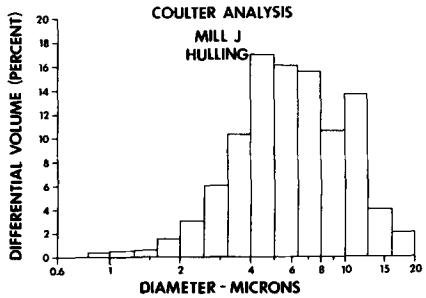

FIG. 10. Typical Coulter analysis histogram of differential percentage total volume distributed by particle diameter.

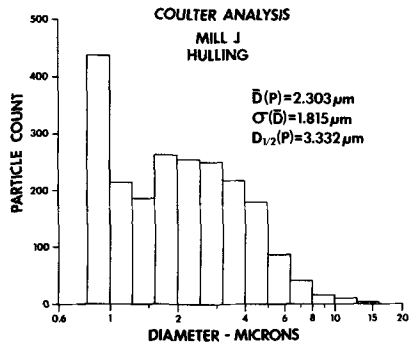

FIG. 9. Typical Coulter analysis histogram of particle count distributed by particle diameter.

in Figure 10. The asymmetric nature of the population data (Fig. 9) transforms into a much more symmetrical distribution than that shown in Figure 3. The Coulter counter data show a peak for $\Delta V(D)$ at about 4.5 μm whereas the image analyzer gives something closer to 19 μm.

Let us now consider the results accumulated by image analysis of VE filter samples collected at various processing locations in 2 different cottonseed oil processing mills (A and J). Both mills were processing seed from stripper-harvested cotton. Mill A used saw delinters exclusively and, although it had installed considerable dust control equipment, it still had several instances of fugitive dust emissions. Time-weighted average VE values at major locations included: cleaning, 1.460 mg/m^3; delintering, 1.509 mg/m^3; hulling, 0.693 mg/m^3; and baling, 1.271 mg/m^3. Mill J, which had one of the most efficient air control systems surveyed, processed seed with first-cut saw and second-cut abrasive delinters. Time-weighted average VE values were, for the most part, significantly less than those at mill A, and included: cleaning, 0.639 mg/m^3; delintering, 0.467 mg/m^3; hulling, 0.888 mg/m^3; and baling, 0.645 mg/m^3. Data on distribution parameters of the particles only (fibers edited out) are summarized in Table I for mill A and in Table II for mill J. For both mills, $\bar{D}(P)$ values are slightly lower in the cleaning and delintering stages than in the later processing stages. In every case, the maximal particle diameter detected is significantly larger than the 15 μm predicted VE cut-off. Likewise, in more than half of the cases, the MMD is also greater than 15 μm, indicating that at least half of the particle volume or mass on the filter is contributed by particles above the predicted VE cut-off.

Particle size distribution data summarized in Table III were obtained from the Coulter counter at the 6 processing locations in mill J (samples from mill A were not obtained on filters compatible with Coulter analysis). With the exceptions of the $D_{1/2}(P)$ and GSD values, all other distribution parameters shown here are significantly lower than those obtained with the image analyzer (Table II). In addition, the MMD values are all below 15 μm. The trend toward larger values of $\bar{D}(P)$ and $D_{1/2}(P)$ is again evident for the post-delintering stages.

These differences between the results of Coulter and image analyses led to the following controlled experiment in which a sample location (hulling) was chosen in mill J. A carbonate membrane filter and also a nitrocellulose filter were both used to collect VE dust for 15 min each during hulling. Standard filter-preparation procedures were used on both filters. In this case, however, the image analyzer was reprogrammed to size the particles in diameter intervals

TABLE I

Image Analysis Particle Parameters from Mill A[a]

Location	$\bar{D}(P)$ (μm)	$\sigma(\bar{D})$ (μm)	$D_{1/2}(P)$ (μm)	$D_M(P)$ (μm)	MMD (μm)	GSD (μm)
Cleaning	3.999	4.424	2.842	135.1	22.0	2.210
Delintering (1st-cut)	3.484	2.504	2.762	28.98	11.82	2.070
Delintering (2nd-cut)	3.691	3.358	2.661	39.79	20.50	2.193
Linter press (1st-cut)	4.654	5.549	2.733	72.16	26.81	1.985
Linter press (2nd-cut)	4.585	5.006	2.794	47.55	24.60	2.076
Hulling	4.392	3.688	3.223	29.54	15.83	1.837

[a]$\bar{D}(P)$, mean particle diameter; $\sigma(\bar{D})$, standard deviation about the mean; $D_{1/2}(P)$, number median diameter; $D_M(P)$, maximal measured particle diameter; MMD, mass median particle diameter; GSD, geometric standard deviation.

TABLE II

Image Analysis Particle Parameters from Mill J[a]

Location	$\bar{D}(P)$ (μm)	$\sigma(\bar{D})$ (μm)	$D_{½}(P)$ (μm)	$D_M(P)$ (μm)	MMD (μm)	GSD (μm)
Cleaning	3.282	2.013	2.950	36.44	11.40	1.836
Delintering (1st-cut)	4.307	2.602	3.837	29.11	11.62	1.901
Delintering (2nd-cut)	3.546	2.487	2.980	49.03	14.05	2.088
Safety shakers	5.181	3.781	4.116	83.62	13.45	1.765
Hulling	5.991	4.268	4.714	38.44	16.20	1.800
Hull beaters/ purifiers	5.561	4.348	3.944	40.97	13.70	1.851
Press room	5.020	3.112	4.605	31.73	13.30	1.773

[a]$\bar{D}(P)$, mean particle diameter; $\sigma(\bar{D})$, standard deviation about the mean; $D_{½}(P)$, number median diameter; $D_M(P)$, maximal measured particle diameter; MMD, mass median particle diameter; GSD, geometric standard deviation.

TABLE III

Coulter Counter Parameters from Mill J[a]

Location	$\bar{D}(P)$ (μm)	$\sigma(\bar{D})$ (μm)	$D_{½}(P)$ (μm)	$D_M(P)$ (μm)	MMD (μm)	GSD (μm)
Cleaning	1.816	1.265	2.354	16.00	5.950	1.889
Delintering (2nd-cut)	1.733	1.196	2.194	16.00	5.150	1.929
Safety shakers	2.035	1.458	2.695	20.2	6.050	1.921
Hulling	2.303	1.815	3.332	20.2	7.590	1.803
Hull beaters/ purifiers	1.974	1.927	2.630	20.2	10.83	2.313
Press room	2.042	1.579	2.785	20.2	7.370	2.020

[a]$\bar{D}(P)$, mean particle diameter; $\sigma(\bar{D})$, standard deviation about the mean; $D_{½}(P)$, number median diameter; $D_M(P)$, maximal measured particle diameter; MMD, mass median particle diameter; GSD, geometric standard deviation.

equivalent to those used by the Coulter. In both cases, the particle count data were adjusted to extrapolate to the total number of particles collected on each filter. These 2 curves are plotted in Figure 11. These data show excellent quantitative agreement in the region between about 3 and 5 μm. In the case of the smaller size (<2 μm) the Coulter equipment gives much higher counts than does the image analyzer, whereas, for the larger particle diameters (>6 μm), the counts fall off much more rapidly for the Coulter than they do for the image analyzer. It is possible that the image analyzer does not measure the small particle as efficiently as the Coulter counter, that some of the small particle counts registered by the Coulter counter may be electronic noise, or that the Coulter counter's sonification preparation procedure shatters a few of the large particles creating many small ones. The differences in the larger particle counts could result from the fact that the equivalent spherical volume assumption of the image analyzer results in an overestimation of the volume of flat particles. Likewise, the Coulter counter's apparent low reading could result from either the shattering phenomena or from errors caused by settling. Nonetheless, these discrepancies and the resulting possibilities lead the author to resolve to do further research in an effort to settle these questions of equivalence between the Coulter counter and the image analyzer.

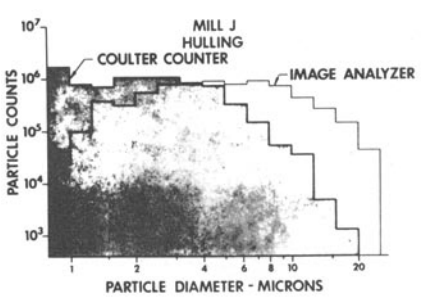

FIG. 11. Comparison of particle count data from equivalent experiments with the image analyzer and the Coulter counter.

The techniques just described for image analysis of cotton fibers and fiber fragments were applied to the sample lots from mills A and J. These data, displayed in Tables IV and V, include the following fiber data: mean length, $\bar{L}(F)$; standard deviation, $\sigma(\bar{L})$; median length, $L_{½}(F)$; maximal detected length, $L_M(F)$; mean width, $\bar{W}(F)$; and standard deviation, $\sigma(\bar{W})$. Several conclusions can be drawn from these data. Obviously, the VE does not sample lint-free dust. In the case of mill A (Table IV), fiber fragments are sampled that are significant fractions between about 0.4 and 0.9 mm in length. On the average, shorter fiber fragments (between 0.2 and 0.3 mm) were found in the mill J samples (Table V). However, in both these cases, fibers were observed that were even longer than a millimeter, approaching a quarter of an inch length. Fiber widths reported in the range of 10-20 μm are quite reasonable for the projected diameters of cotton lint.

One of the primary objectives ot this study has been to characterize the VE-sampled oil mill dust to distinguish the relative amount of nonlint particulates from the fibrous or linty fraction and to develop a quantitative relationship between the two. Up to this point, the data presented have

TABLE IV

Image Analysis Fiber Parameters from Mill A[a]

Location	$\bar{L}(F)$ (μm)	$\sigma(\bar{L})$ (μm)	$L_{½}(F)$ (μm)	$L_M(F)$ (μm)	$\bar{W}(F)$ (μm)	$\sigma(\bar{W})$ (μm)
Cleaning	743.2	580.8	625.3	2,650	23.13	10.62
Delintering (1st-cut)	401.3	726.1	280.3	6,648	10.82	6.974
Delintering (2nd-cut)	486.5	572.6	343.8	3,952	15.37	11.39
Linter press (1st-cut)	427.9	798.3	184.8	5,553	12.63	7.254
Linter press (2nd-cut)	857.1	774.4	618.1	5,025	16.68	15.22
Hulling	897.4	735.1	739.8	4,679	18.26	7.192

[a]$\bar{L}(F)$, mean length; $\sigma(\bar{L})$, standard deviation; $L_{½}(F)$, median length; $L_M(F)$, maximal detected length; $\bar{W}(F)$, mean width; $\sigma(\bar{W})$, standard deviation.

TABLE V

Image Analysis Fiber Parameters from Mill J[a]

Location	$\bar{L}(F)$ (μm)	$\sigma(\bar{L})$ (μm)	$L_{½}(F)$ (μm)	$L_M(F)$ (μm)	$\bar{W}(F)$ (μm)	$\sigma(\bar{W})$ (μm)
Cleaning	338.8	562.5	187.5	3,061	17.60	8.23
Delintering (1st-cut)	194.9	151.1	164.2	796	15.77	6.01
Delintering (2nd-cut)	256.7	250.6	184.4	1,219	17.78	8.33
Safety shakers	316.1	797.9	148.1	6,159	14.48	6.44
Hulling	316.1	382.2	183.8	2,346	20.67	8.74
Hull beaters/ purifiers	315.4	364.9	193.2	1,765	19.96	5.32
Press room	265.2	321.8	168.7	2,322	15.24	7.01

[a]$\bar{L}(F)$, mean length; $\sigma(\bar{L})$, standard deviation; $L_{½}(F)$, median length; $L_M(F)$, maximal detected length; $\bar{W}(F)$, mean width; $\sigma(\bar{W})$, standard deviation.

TABLE VI

Relative Contributions of Particles and Fibers in Samples from Mill A

Location	$A_f(P)$	$A_f(F)$	$V_f(P)$	$V_f(F)$	FAF[a]	FVF[b]
Cleaning	0.088	0.024	2.319	0.496	0.218	0.176
Delintering (1st-cut)	0.051	0.023	0.326	0.171	0.308	0.344
Delintering (2nd-cut)	0.052	0.021	0.533	0.157	0.173	0.227
Linter press (1st-cut)	0.035	0.019	0.563	0.132	0.344	0.190
Linter press (2nd-cut)	0.028	0.025	0.383	0.147	0.465	0.278
Hulling	0.020	0.019	0.180	0.119	0.488	0.400

[a]FAF, fiber area fraction $= \frac{A_f(F)}{A_f(P) + A_f(F)}$.

[b]FVF, fiber volume fraction $= \frac{V_f(F)}{V_f(P) + V_f(F)}$.

principally been of a relative nature and by no means have been quantitative or absolute. The image analyzer allows for using 2 different types of comparison between particles and fibers based on either their directly measured areas or inferred volumes. Besides accumulating histogram-type distribution data for features measured over numerous fields of view, the image analyzer can also be programmed to measure the sum of any one feature parameter (such as its area) over all features in a single frame and then over all frames. By dividing this quantity by the sum of the measurement-frame areas, the analyzer gives the fraction (A_f) occupied by the features measured. Similarly, the feature parameters of equivalent spherical volume, V_{es} (as defined in Eq. II), can be used to calculate the total particle volume per substrate area scanned (that is, the feature volume fraction, V). These quantities are included in both the particle- and fiber-measuring programs and will be called $A_f(P)$ and $V_f(P)$ for the particles and $A_f(F)$ and $V_f(F)$ for the fibers. These 4 parameters are listed in Tables VI and VII for the various processing locations of mills A and J, respectively.

TABLE VII

Relative Contributions of Particles and Fibers in Samples from Mill J

Location	$A_f(P)$	$A_f(F)$	$V_f(P)$	$V_f(F)$	FAF[a]	FVF[b]
Cleaning	0.141	0.028	0.927	0.263	0.166	0.221
Delintering (1st-cut)	0.131	0.019	0.791	0.118	0.126	0.130
Delintering (2nd-cut)	0.096	0.017	0.818	0.136	0.150	0.143
Safety shakers	0.391	0.025	2.848	0.244	0.061	0.073
Hulling	0.155	0.021	1.456	0.185	0.119	0.113
Hull beaters/ purifiers	0.176	0.012	1.544	0.090	0.066	0.055
Press room	0.254	0.024	1.818	0.190	0.084	0.091

[a]FAF, fiber area fraction $= \frac{A_f(F)}{A_f(P) + A_f(F)}$.

[b]FVF, fiber volume fraction $= \frac{V_f(F)}{V_f(P) + V_f(F)}$.

Also included are the area and volume fractions of fiber calculated per total (particles plus fiber) area and volume, respectively. Because the area and volume fractions for the various samples have not been normalized to account for differences in sampling time, comparisons cannot be made between A_f and V_f values among the different samples. However, the sampling times cancel out in the calculation of the fiber contribution (area and volume) factors. In general, both of these factors have close to the same values and show similar trends. Although there appears to be no definite trend or correlation of these factors with respect to processing location, it appears that the values for mill A are substantially larger than for mill J. This fact, coupled with the larger fiber fragments reported for mill A, indicate that the lower efficiency dust control system allows significantly larger quantities of airborne lint or fly than does the improved system in mill J.

Careful consideration of the data leads one to the following observations: (a) air-borne dust sampled by a vertical elutriator in cottonseed oil mills is not limited to nonlint dust less than 15 μm in diameter. In many cases, a considerable fraction of the total dust accumulated is attributed to lint and lint fragments, as well as to particles greater than 15 μm in diameter; (b) there is an apparent trend in both mills for the average diameter of nonlint particles to increase in the processing stages following delintering; (c) the average length and relative amount of lint fragments present on the VE filters appear to correlate with the elevated dust concentrations measured in mill A and to be significantly reduced by the dust control system in effect in mill J; and (d) there is a definite discrepancy between the size distribution data generated with the Coulter counter and the analysis of the same dust with a microscopic image-analysis system.

ACKNOWLEDGMENTS

Several individuals provided cooperation and assistance in this work: R.M. Bethea collected the VE samples and gave many helpful discussions, J. Evans prepared microscope samples and made the image analysis, and S. Armand prepared samples and made Coulter counter analyses.

Memorandum of Agreement 58-7B30-9-123 between USDA and the Texas Tech University, R.M. Bethea, principal investigator, Sept. 1979.

REFERENCES

1. Neefus, J.D., J.C. Lumsden and M.T. Jones, Am. Ind. Hyg. Assoc. J. 38:394 (1977).
2. National Institute for Occupational Safety and Health: Criteria for a recommended standard; Occupational Exposure to Cotton Dust. (HEW, Pub. no. [NIOSH] 75-118) 117 (1974).
3. Matlock, S.W., L.R. Wiederhold, Jr., and C.B. Parnell, Jr., Trans. Am. Soc. Agric. Eng. 19:970 (1976).
4. Matlock, S.W., and C.B. Parnell, Jr., Proc. ASME Textile Engineering Division Conference, 1976, paper no. 76-TEX-10.
5. Parnell, C.B., Jr., and S.W. Matlock, Proc. 1977 Special Session Cotton Dust-Beltwide Cotton Production Conference, Atlanta, GA, 1977.
6. Parnell, C.B., Jr., Evaluations of Engineering Controls for Cotton Dust in Oil Mills, Final Report, Cooperative Agreement No. 58-7B30-8-44, Texas A&M University, 1979.
7. Bethea, R.M., and P.R. Morey, American Conference of Government Industrial Hygienists' National Cotton Dust Symposium, Atlanta, GA, 1974.
8. Claassen, B.J., Jr., Am. Ind. Hyg. Assoc. J. 40:993 (1979).
9. Neefus, J.D., Ibid. 36:475 (1975).
10. Robert, K.Q., Jr., Ibid. 40:535 (1979).
11. Swenson, R.A., and J.R. Attle, Am. Lab. 11:50 (1979).